CALCULATION OF PROPAGATION LOSSES IN A MEDIUM WITH A VELOCITY PROFILE APPROXIMATED BY A NUMBER OF EPSTEIN PROFILES

by

T. Strarup

Danish Defence Research Establishment

Copenhagen, Denmark

ABSTRACT

This paper presents a digital ray-theory program, by which the ray trace, travel time and intensity can be calculated for velocity profiles approximated by a number of Epstein functions.

INTRODUCTION

In order to extract information from underwater acoustic propagation measurements the Danish Defence Research Establishment have started an investigation on calculation of propagation losses in a medium with a given sound velocity profile. The object is to calculate propagation losses with reasonable accuracy by a method which requires a limited computer capacity. In order to obtain reasonable accuracy by using relatively few approximating functions for the sound velocity profile, symmetrical Epstein profiles were chosen. In this way the profile approximation is a continuous function with a continuous first derivative and, moreover, the mathematical problems are much simplified, as will be seen in the following.

The problems related to the curve fitting procedure will not be mentioned here. At the moment the curve fits are made by means of a combined manual and digital procedure which, however, will be improved in the future at DDRE.

A SHORT DESCRIPTION OF THE PROGRAM

The first four figures show the capability of the program. Figure 1 is a plot of a velocity profile approximated by two Epstein functions which join at a depth of 40 m. Figure 2 shows the ray-trace from a transmitter placed at a depth of 5 m and with a beamwidth of 20°. The travel time at 900 m distance is shown in Fig. 3. The sign ∿ indicates the starting point, which corresponds to the steepest upgoing ray from the transmitter. The plot indicates four wave fronts arriving at $x = 900$ m with travel times $0.6345 < t < 0.6365$ s. Figure 4 shows the propagation losses at $x = 900$ m and at 1 kHz. They are calculated by a vectorial addition of the separate arrivals. A reflection coefficient of $r = 1$ is assumed at the surface, not in accordance with reality. However, it should be mentioned, that the program can accept an arbitrary value for r as well as an arbitrary radiation pattern from the transmitter.

In Fig. 5 is shown the mathematical expression for a symmetrical Epstein function and our definition of the ray-parameter p from Snell's law, which makes the mathematical expressions practical for both upgoing and downgoing rays.

Figures 6 and 7 show the simplicity of the mathematical formulae $x = f(z)$ and $t = f(x,z)$.

The above-mentioned formulae are valid only in the first quarter of a ray-trace period. Figure 8 shows how it is possible for an arbitrary x to transform x to a value where the formulae mentioned are valid.

An outline of the program is given in Fig. 9.

CONCLUSIONS

In a way there is no conclusion of this paper, so far. In order to obtain a conclusion, it is necessary to:

1. Compare some of our outputs with outputs from other ray-theory programs.
2. Investigate the computer capacity required by solving hard problems.
3. Finish the work concerning curve fitting.

DISCUSSION

In response to questions, the author explained the technique of fitting Epstein profiles to a given sound speed profile as first fitting the upper and lower portions, then the centre portion by an Epstein profile which preserved a continuous first derivative across the two boundaries. He found the display of depth, travel time, intensity, etc., as functions of range a convenient method of presenting the results, but had no strong feelings about this.

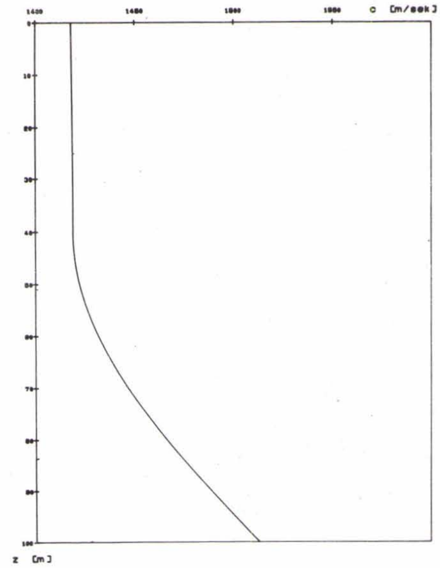

FIG. 1

'ydhastighedsprofil: februar 3

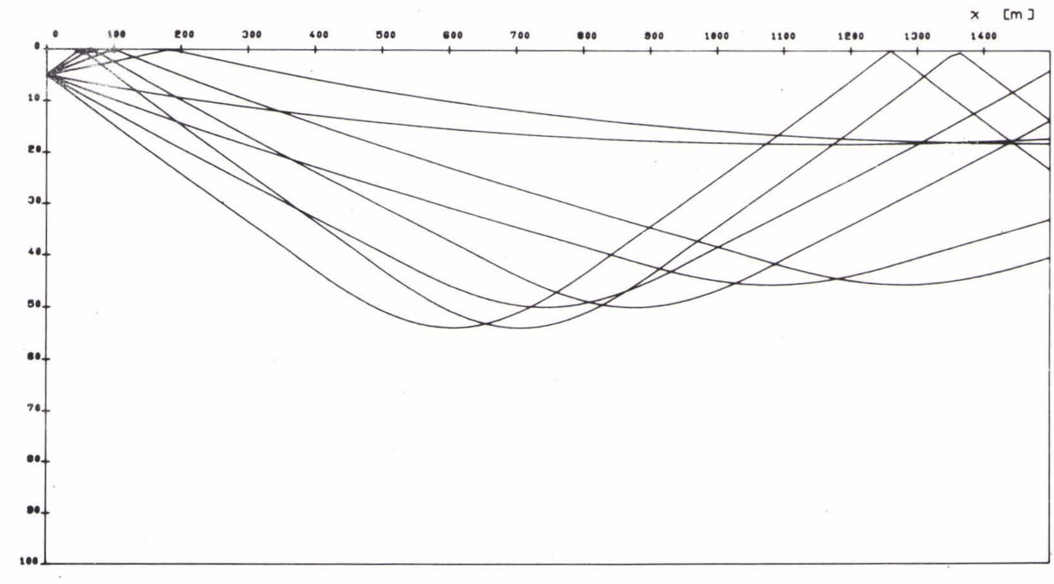

raytracing med profil: februar 3

FIG. 2

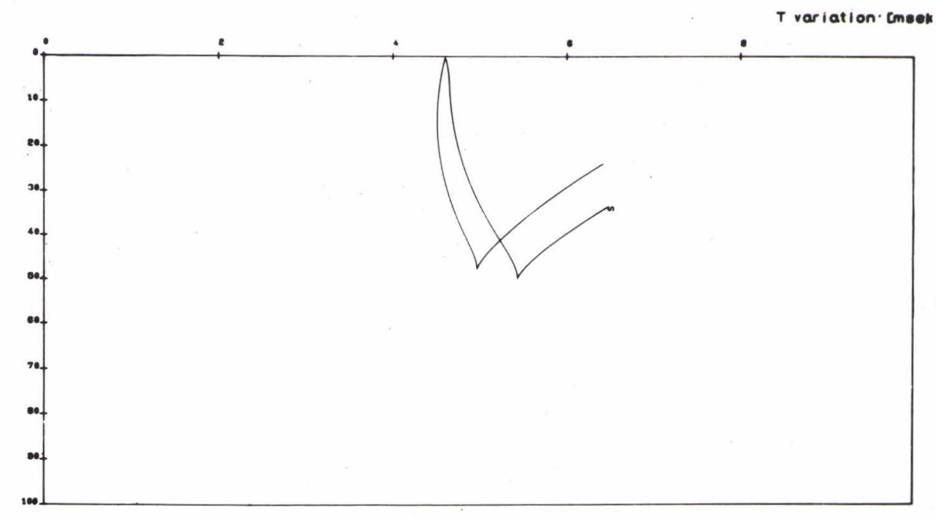

FIG. 3

T-Z plot, profil= februar 3

tmin= 0.63 sek

x= 900 m

FIG. 4

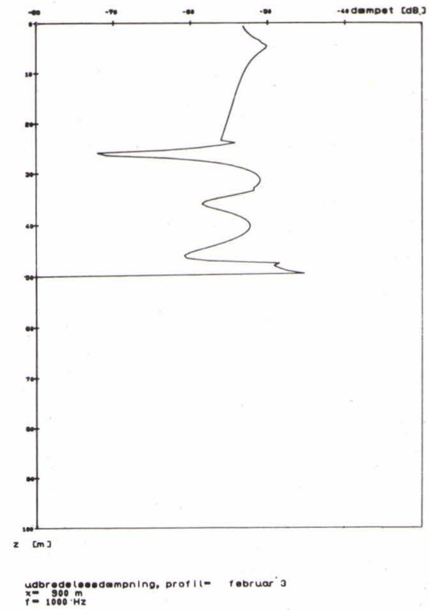

The soundvelocity profile is approximated by a number of Epstein Profiles.

$$C_n(z) = \frac{1}{\sqrt{A_n \, tgh^2 \frac{z - z_{cn}}{H_n} + B_n}}$$

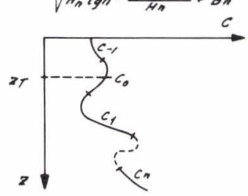

FIG. 5

Snells law:

$$\frac{\sin\theta}{C_0} = \frac{\sin\theta_n}{C_n} = p$$

$p = \frac{\sin\theta_0}{C_0}$ for $0 < \theta_0 < \frac{\pi}{2}$ and

$p = -\frac{\sin\theta_0}{C_0}$ for $\frac{\pi}{2} < \theta_0 < \pi$

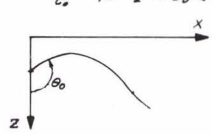

FIG. 6

$$x = p\int_{z_1}^{z} \frac{dz}{\sqrt{C(z)^{-2} - p^2}}$$

$$= p\int_{\sinh\frac{z_1 - z_0}{H}}^{\sinh\frac{z - z_0}{H}} \frac{du}{\sqrt{(A+B-p^2)u^2 + B - p^2}}$$

I: $B - p^2 > 0$ and $A + B - p^2 < 0$

$$x = \frac{pH}{b}\sin^{-1}\left(\frac{b}{a}\sinh\frac{z - z_0}{H}\right) - x_1$$

where $a = \sqrt{|B - p^2|}$ and

$b = \sqrt{|A + B - p^2|}$

II: $B - p^2 > 0$ and $A + B - p^2 > 0$

$$x = \frac{pH}{b}\sinh^{-1}\left(\frac{b}{a}\sinh\frac{z - z_0}{H}\right) - x_1$$

III: $B - p^2 < 0$ and $A + B - p^2 > 0$

$$x = \frac{pH}{b}\cosh^{-1}\left(\frac{b}{a}\sinh\frac{z - z_0}{H}\right) - x_1$$

$$t = \int_{z_1}^{z} \frac{C(z)^{-2}}{\sqrt{C(z)^{-2}-p^2}}\,dz$$

$$= \frac{(A+B)x}{|p|} + \frac{pH}{|p|}\int_{tgh\frac{z_1-z_0}{H}}^{tgh\frac{z-z_0}{H}} \frac{-A\,du}{\sqrt{Au^2+B-p^2}}$$

FIG. 7

<u>$TI:\ A<0$</u>

$$t = \frac{A+B}{|p|}x + H\,sign(p)\sqrt{|A|}\,\sin^{-1}\left(\sqrt{\frac{|A|}{|B-p^2|}}\,tgh\,\frac{z-z_0}{H}\right) - t_1$$

<u>$TII:\ A>0$</u>

$$t = \frac{A+B}{|p|}x + H\,sign(p)\sqrt{|A|}\,\sinh^{-1}\left(\sqrt{\frac{|A|}{|B-p^2|}}\,tgh\,\frac{z-z_0}{H}\right) - t_1$$

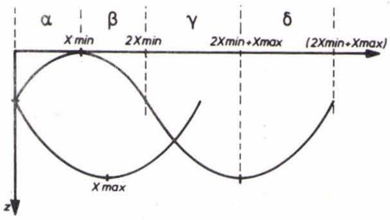

Interval α:

$z(x) = \varphi(x)$

$t(x) = \Psi(x)$

Interval β:

$z(x) = \varphi(2x_{min} - x)$

$t(x) = 2t_{min} - \Psi(2x_{min} - x)$

Interval γ:

$z(x) = \varphi_1(x - 2x_{min})$

$t(x) = 2t_{min} + \Psi_1(x - 2x_{min})$

Interval δ:

$z(x) = \varphi_1[2(x_{max} + x_{min}) - x]$

$t(x) = 2t_{min} + 2t_{max} - \Psi_1[2(x_{max} + x_{min}) - x]$

FIG. 8

FIG. 9

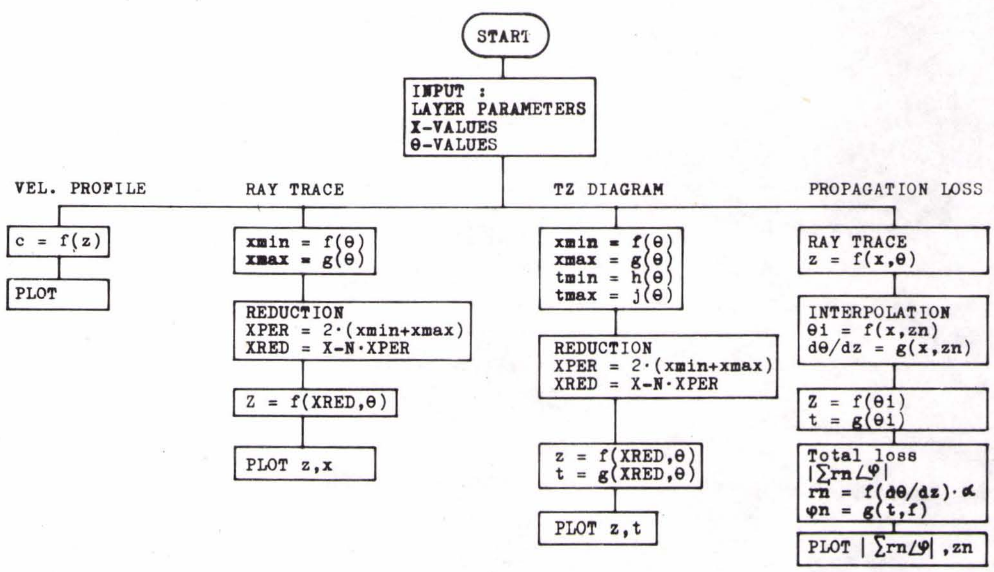

OUTLINE